



Using Lidar DEM to Map Landslides: Škofjeloško Cerkljansko Hills, Slovenia

Erazem Dolžan and Mateja Jemec Auflič

Abstract

LiDAR has become an effective tool in landslide research, particularly in landslide mapping. While applicability of LiDAR and its derivative products has already been proven for identification of historical landslides worldwide, mapping shallow landslides triggered during stormy periods presents a greater challenge to landslide investigators. The main objective of the present study is landslide identification using Lidar DEM in the Škofjeloško Cerkljansko area, characterized by diverse morphology, dense vegetation cover and historical landslide records. Altogether 114 landslides were mapped using Lidar-derived hillshades, correlated with PSInSAR data, landslide database and a limited sample was later verified in the field. Field validation was limited due to steep, inaccessible terrain covered by forest. However, this study suggests that DEM analysis can remotely provide information about possible landslide activity and can help land managers in reducing landslide risk and avoiding potential disasters. But at the moment, little chance of automatizing the process is seen, as the landforms determined as indicative of landsliding, especially for the slope instabilities of smaller dimensions, are difficult to delineate without subjective expert opinion.

Keywords

Mapping landslides • Lidar • Landslide identification • Landslide inventory

Introduction

Mapping landslide inventories in areas with dense vegetation is difficult, as demonstrated by a number of authors (e.g. Schulz 2004; Van Den Eeckhaut et al. 2007; Kasai et al. 2009). Most remote sensing methods normally used to detect landslide features are severely hindered by the vegetation cover. While field investigations can usually give good results, they are often costly, time-consuming and logistically complicated. Airborne laser scanning (ALS), also

known as Lidar, presents an effective method for quick evaluating the topography and landslide mapping in such areas (McKean and Roering 2004; Glenn et al. 2006; Guzzetti et al. 2012; Jaboyedoff et al. 2012; Razak et al. 2013). Its ability to filter points belonging to vegetation and display a “bare Earth model” is invaluable in detecting topographic features indicative of landsliding and makes Lidar a valuable tool for landslide inventory mapping in forested areas, especially when combined with other types of data and fieldwork. It is particularly valuable in identifying and mapping deep landslides that are often difficult to detect by other means. Moreover, a landslide inventory map, which shows the location of landslide phenomena and contains information about movement type, activity, etc., is a basic element for landslide susceptibility and risk assessment (Schulz 2006; Van Westen et al. 2008; Van Den Eeckhaut et al. 2007; Guzzetti et al. 2012).

E. Dolžan (✉)
Kropa 11, 4245 Kropa, Slovenia
e-mail: Erazem.dolzan@gmail.com

M. Jemec Auflič
Geological Survey of Slovenia, Dimičeva ulica 14,
1000 Ljubljana, Slovenia
e-mail: mateja.jemec@geo-zs.si

In Slovenia, an important step in using Lidar Data for identification surface morphology was done by Podobnikar (2005). Recently, Popit et al. (2013), Popit and Verbovšek (2013) and Popit et al. (2014) demonstrated application of surface roughness to identify fossil landslides in Vipava valley. In general, LiDAR is particularly effective in identifying presumably older landslides and the boundaries of complexes in which recently active landslides occur.

In this work, we will focus on landslide identification using Lidar DEM in the Škofjeloško Cerkljansko area, characterized by diverse morphology, dense vegetation cover and historical landslide records.

Study Area

Our study area lies in Škofjeloško Cerkljansko hills located in the western central part of Slovenia, northwest of the capital city Ljubljana (Fig. 1). It covers approximately 580 km². Geomorphologically, it is characterized by Alpine foothills, where the altitude difference between summits and valleys is mostly in the order of 100 s of meters, with altitudes above sea level spanning between 300 m to over 1600 m. High slope angles are also characteristic of this area; slopes can reach 30°–40° or be even steeper. In terms of lithology, the area is composed largely of two types of rocks, Mesozoic carbonate rocks and Palaeozoic clastic rocks, ranging from quartz conglomerate to claystone (Buser et al. 1968). The latter in particular are very susceptible to landsliding and form many parts of Slovenia where landslide hazard is high. While the Mesozoic carbonate usually forms fairly stable slopes, it also forms cliffs, which present rockfall hazard, and major talus slopes and scree deposits which can present source material for further landslides, especially in combination with weak and weathered clastic rocks. The investigated area is covered by temperate mixed forest and meadows. The two dominating tree species in the forest are beech and spruce, with fir and several deciduous species occupying a smaller percentage. Major urban areas are limited to valley and basin floors, with only smaller settlements and solitary farms occupying the hill slopes.

Landslides in the study area usually occur due to particular weather conditions with heavy rainfall (Jemec Auflič and Komac 2013). Over the period between 1990 and 2010, approximately 492 landslides have been recorded from the Slovenian National landslide database (Komac et al. 2007), technical reports and bulletins (Administration for Civil Protection and Disaster Relief), and from annual reports by Ujma from 1991 to 2010 (Jemec Auflič et al. 2015). In 2007, the study area was hit by an intense storm event that claimed six lives. Jemec Auflič and Mikoš (2008) used SPOT satellite images for identification of landslide types triggered after the event.

Data and Methodology

Lidar Data

The Lidar data used in our study was collected in a nation-wide laser scanning campaign, carried out between 2011 and 2015, with most of Slovenia being scanned between February 2014 and April 2015. The data acquisition and processing was carried out by Slovenian company Flycom d.o.o. (<http://www.flycom.si/#home>), under the direction of the Geodetic Institute of Slovenia. Triglav Čekada and Bric (2015) present an overview of the completed project. Nominal point density of the scans was 5 pts/m² across most of the territory, with a density 2 pts/m² over the larger forested areas. Quality control on the finished products concluded that the data exceeded the initial accuracy benchmarks of 0.3 m for positional accuracy and 0.15 m for vertical accuracy (Triglav Čekada and Bric 2015).

In the present study, a High Resolution Digital Elevation Model (HRDEM) with a horizontal resolution of 1 m, produced from the laser scanning point cloud, was used. The regular grid of HRDEM was easier to handle than the classified point cloud, given the size of the study area and available software and hardware. The 1 m resolution should be large enough to distinguish typical landsliding features.

Lidar Derivatives and Landslide Mapping

Our approach to mapping was similar to one described by Schulz (2006). A number of derivatives were created from the original Lidar data to facilitate mapping. First of all, hillshades with different light directions were prepared, in our case using light dip of 45° and azimuths of 45°, 75°, 135°, 220° and 315°. The large number of different light azimuths proved invaluable, because the relief of the area is very rugged and many slopes would appear either shaded or blown out on single hillshade map, making any minor geomorphological features hard to see. As a result, potential landslide features would appear drastically different when viewed in different light directions (Fig. 2) and often had to be examined in multiple hillshades, before they could be mapped with any certainty. A slope map was also prepared in order to help differentiate areas potentially more prone to landsliding.

Additionally, a surface roughness map and a Topographic Ruggedness Index (TRI) maps were prepared. Both roughness maps and TRI maps determine the variability of a surface by comparing the raster value of a certain point with its neighbours. In theory, landslide areas should display higher surface variability than surrounding terrain, due to the presence of scarps, cracks, hummocky terrain etc. While

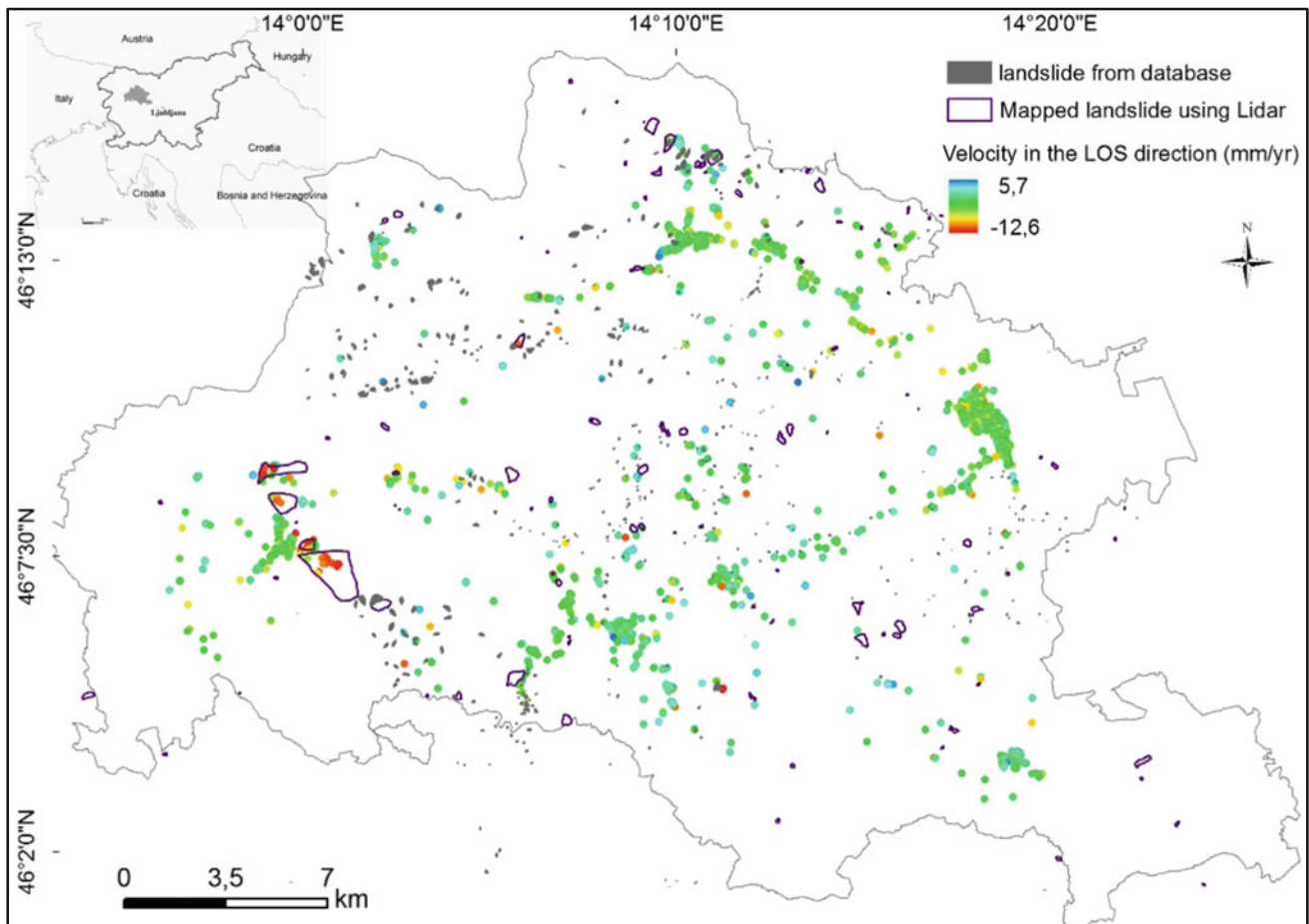


Fig. 1 Location of the study area, including landslides mapped using Lidar data and landslides from database. PS points are marked on the map and ranged by velocity in mm/year

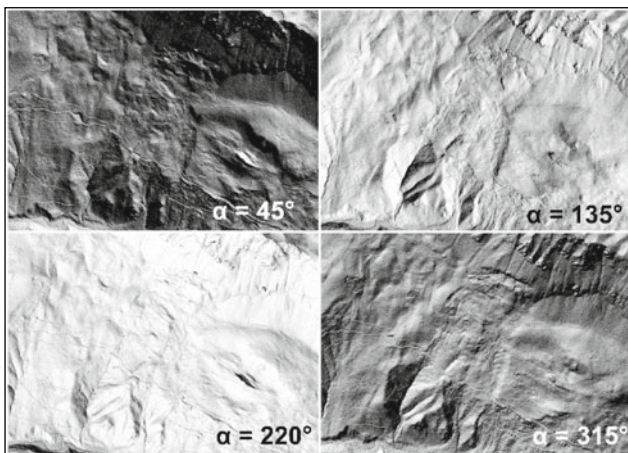


Fig. 2 Hillshade representations of a potential landslide feature near Dražgoše under different light directions. Note the relatively dark image at an azimuth of 45° and blown-out look with almost no details visible at 220° . Landslide features are usually best visible when the light direction is roughly parallel to the strike of the slope

various surface roughness analyses were successfully used in landslide mapping and characterisation by a number of authors (e.g. McKean and Roering 2004; Liu et al. 2012; Li et al. 2015), even using automatic or semi-automatic mapping methods, the surface roughness in our case reflects land use, slope angle and aspect and underlying geology more than features, related to landslides. Forests would generally show higher roughness than meadows and the highest values would appear on the steepest, partly rocky slopes. Overall, hillshade maps proved to be by far the most useful Lidar derivative for landslide mapping and were used as the main source for mapping. Orthorectified RGB aerial imagery was used to supplement Lidar derivatives, primarily to distinguish manmade features from potential landslide features and sometimes provide additional details in non-forested areas.

Lidar derivatives were prepared using the open source geoprocessing library OSGeo and the entire dataset was organised and collected into a GIS environment using the

QGIS software package, in which the landslide mapping was also carried out.

The area was mapped by systematically panning over the entire area at different magnifications and mapping was typically carried out at a higher magnification in order to better delineate the landslide features. Landslides were mapped on the basis of distinct morphological characteristics, including head scarps, toe features, hummocky terrain, convex-concave features etc. Among those, head scarps were usually most prominent (and abundant), but were not considered as sufficient evidence to map landslides with certainty as there were many features visually similar to head scarps visible on hillshades. Only when head scarps were combined with other morphological characteristics we were able to determine a landslide with any certainty. In key areas, altitude profiles were created over the investigated features to aid in determination.

Along with the geometry of a potential landslide, its type (where possible) was recorded. A certainty value from 1 to 5 was also given to every landslide, 5 being the most certain and 1 the least. Using a certainty scale enabled us to record a larger number of features even if their origin was uncertain and not necessarily connected to landsliding. While this may lead to a number of false positives being mapped, it also allows us to compare different features both related to landsliding and not, on Lidar hillshades and in the fields, in order to learn how to see the differences between them.

Field Work—Ground Proofing

A limited sample of the landslides mapped were later examined in the field. The landslides to be included in the sample were as diverse as possible; we tried to visit as many different forms as we could in order to get a better insight into the relationship between what is visible on the hillshades and in the field. Logistical considerations also played a part in choosing the sample landslides, as priority was given to locations in proximity of roads or otherwise easily accessible.

In the field, typical signs of landslide activity not visible on Lidar, such as pistol-butt trees, cracks in the ground and tree roots under tension, springs and wetlands indicating a change in the ground water regime etc. were observed. Furthermore, a comparison between morphological features observed in the field and on the hillshades was made (Fig. 3).

PSInSAR Data

The mapped landslide features were compared with Permanent Scatterer Interferometric Synthetic Aperture Radar

(PSInSAR) data. PSInSAR is a powerful remote sensing technique able to measure displacements of the Earth's surface (Ferretti et al. 2001; Colesanti et al. 2003; Crosetto et al. 2016). Permanent scatterers can be natural, e.g. rock outcrops, or artificial, such as buildings, bridges, dams, antennas, and similar objects (Ferretti et al. 2001). Also intentionally constructed scatterers may be used, like simple metallic plates or rectangular reflectors. For the study area, the PSInSAR data were collected and analysed by Jemec Auflič (2012). In total, 67 SAR images were used, spanning a period from 1992 to 2000. From these, 2786 permanent scatterers were determined (Fig. 1). Most of the scatterers are situated in urban areas in the valleys and were therefore of little use, but a few were located on the mapped landslides and provided verification of the activity of certain landslides.

Results and Discussion

In total, landslide mapping using Lidar revealed 114 features resembling landslides within the study area. Among them, 15 were attributed a certainty value of 1 (i.e. the lowest value) and are possibly other landforms similar to landslides. 38 were attributed values of 4 or 5 and are almost certainly landslides.

However, only 15 of the landslides were checked in the field so far. Signs of current or former slope instability were discovered on 10 of these, while 5 were found to display little or no signs of instability. This means a success rate of just 66%. Furthermore, 4 new landslides of sufficient size that they should be visible on Lidar were discovered in the field but were missed during Lidar mapping. Traces of one (Fig. 4a, b) were visible on Lidar, but it was probably missed due to its small size, while the other showed very little trace. Two may be too shallow (mostly shallower than 0.5 m) to be visible on Lidar (Fig. 4c, d). One was a debris flow that was almost certainly triggered after the area was scanned. The results of the field validation so far are not encouraging, however, bear in mind that a very small sample was checked in the field so far. In the future, we hope to carry out a more detailed field validation in order to check a larger number of mapped landslides and at the same time map systematically map a part of the area to get an idea on how many landslides may have been missed by the Lidar mapping. Partly, the low success rate may also be down to mapping more features to be later examined in the field. These would normally not be included in an inventory mapping project, but we included them here in order to compare them in the field and learn to detect the difference.

In general, landforms indicative of landsliding were visible on Lidar in great detail and could be easily located in the field. In some areas however a field examination revealed additional detail or caused us to reconsider our interpretation

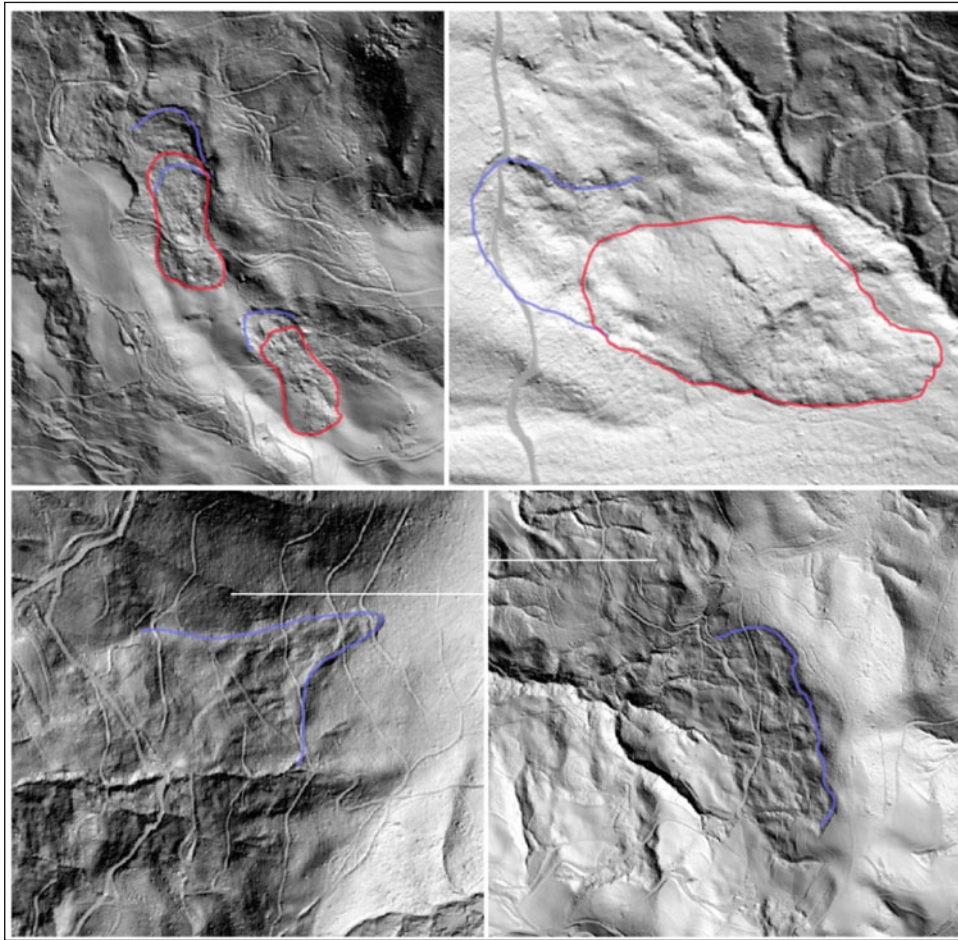


Fig. 3 Landslide forms as seen on Lidar-derived hillshades. *Top* Scarps, landslide bodies and toe features, typical concave-convex profiles. *Bottom* Head scarps and hummocky terrain, indicative of deep-seated slow moving deformations

(often to include features we originally dismissed as unimportant). For example, Fig. 5 shows a fairly distinctive landslide (marked 5 on the certainty scale) that was later examined in the field. Field examination showed that most of the landslide was currently inactive, with the exception of a few fresh cracks on the head scarp (Fig. 5a). However, the most active part of the landslide proved to be a secondary scarp that formed uphill from the main scarp (Fig. 5b) and was initially dismissed during mapping.

Lidar proved to be particularly effective in mapping deep-seated slow-moving slope instabilities (Fig. 3 Bottom). Rockfall areas were also clearly visible due to prominent steep cliffs and scree slopes, but could easily be confused with a number of small-scale quarries present in the area. Aerial imagery was normally sufficient to tell them apart.

One major difficulty in the mapping was determining the activity of the landslide forms observed on the hillshades, as we find that landslide form do not decay as linearly with time as we would expect and some older and completely

inactive display clear and crisp morphology despite being inactive for a long time. Figure 6 shows such an example, where the form of the landslide was clearly defined, but was found to be overgrown by undeformed trees and therefore inactive for quite some time. In some cases, it was possible to infer activity based on damage to the roads crossing the landslide (e.g. Fig. 5a), but in many cases (e.g. Fig. 4c) the information may be inconclusive. Road damage may be present, but not necessarily visible on Lidar.

Comparison with PSInSAR Data

To obtain information on activity of the mapped landslides, the landslides were compared to PSInSAR velocities in this area. Out of almost 2800 PS points situated in this area, 74 are located on bodies of the landslides we mapped and out of 117 landslides mapped in total (including the ones discovered during field work), 10 contained at least one PS point.

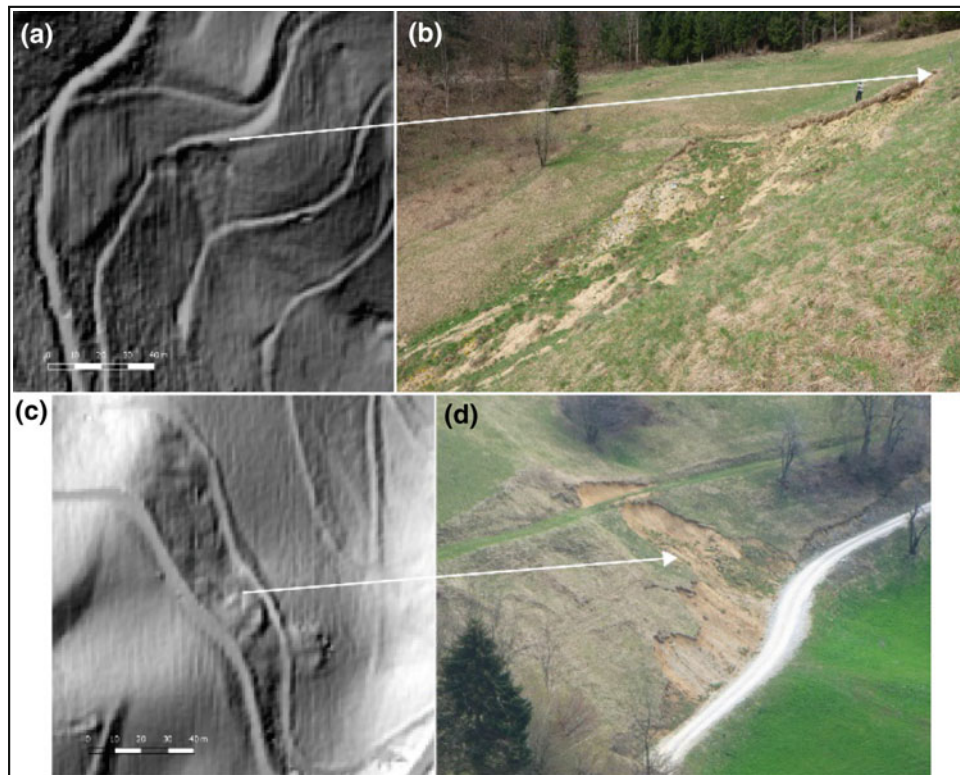


Fig. 4 Landslides on Lidar-derived hillshades and in the field

Better coverage is hard to achieve, as most potential PS points are usually located in urban areas, while the landslides are overgrown by forest.

On average, there is a distinct difference in PS velocities between points situated on the mapped landslide bodies and points situated elsewhere. Typically, points on the surface of landslide bodies present higher velocities (indicative on creeping).

Figure 7a shows velocity histograms for all PS points in the area and Fig. 7b shows points located on landslide bodies. The mean velocity for all points is 0.099 mm/year. By contrast, the mean velocity for points located on the landslide bodies is -3.76 mm/year. Therefore, it can be shown that PSInSAR data display higher rate of slope movements in landslide mapped areas than displacement rates of PS points on stable areas.

Areas that displayed highly negative PSInSAR velocities (i.e. negative is mean that PS points moving away from the satellite and positive moving toward the satellite) typically displayed signs of slope instability as well, mostly hummocky terrain accompanied by head scarps in some places. An exception occurred in the area of the Žirovski vrh uranium mine (now in closing), where high velocities were detected and previous field work (Čarman et al. 2014) indeed defined an unstable area, but no features indicative of

landsliding were visible on the hillshades. This example serves to illustrate that, while Lidar can be a good tool for landslide mapping, not all unstable areas can be detected using only Lidar. Inventory mapping campaigns should therefore combine data from different sources to get a more complete picture.

Evaluation of the Landslide Database

Landslides recorded in this area in the landslide database maintained by the Geological Survey of Slovenia were also reviewed in the course of this study (Fig. 1). Out of 492 landslides recorded in the database, only 59 (12%) exhibited distinctive landslide morphology, visible on Lidar. This percentage is very low, which is probably due to the fact that (1) all landslides cannot form typically shapes clearly visible and recognised on Lidar-derived hillshades, (2) landslides were triggered in the past and not caused major changes in the surface, and (3) landslides are small in size ($200\text{--}1200\text{ m}^3$). Besides the morphology and location of some landslides (on flatland, on both sides of a valley or a ridge etc.) throws doubt on their validity and perhaps exposes the need for a full-scale validation of the database.

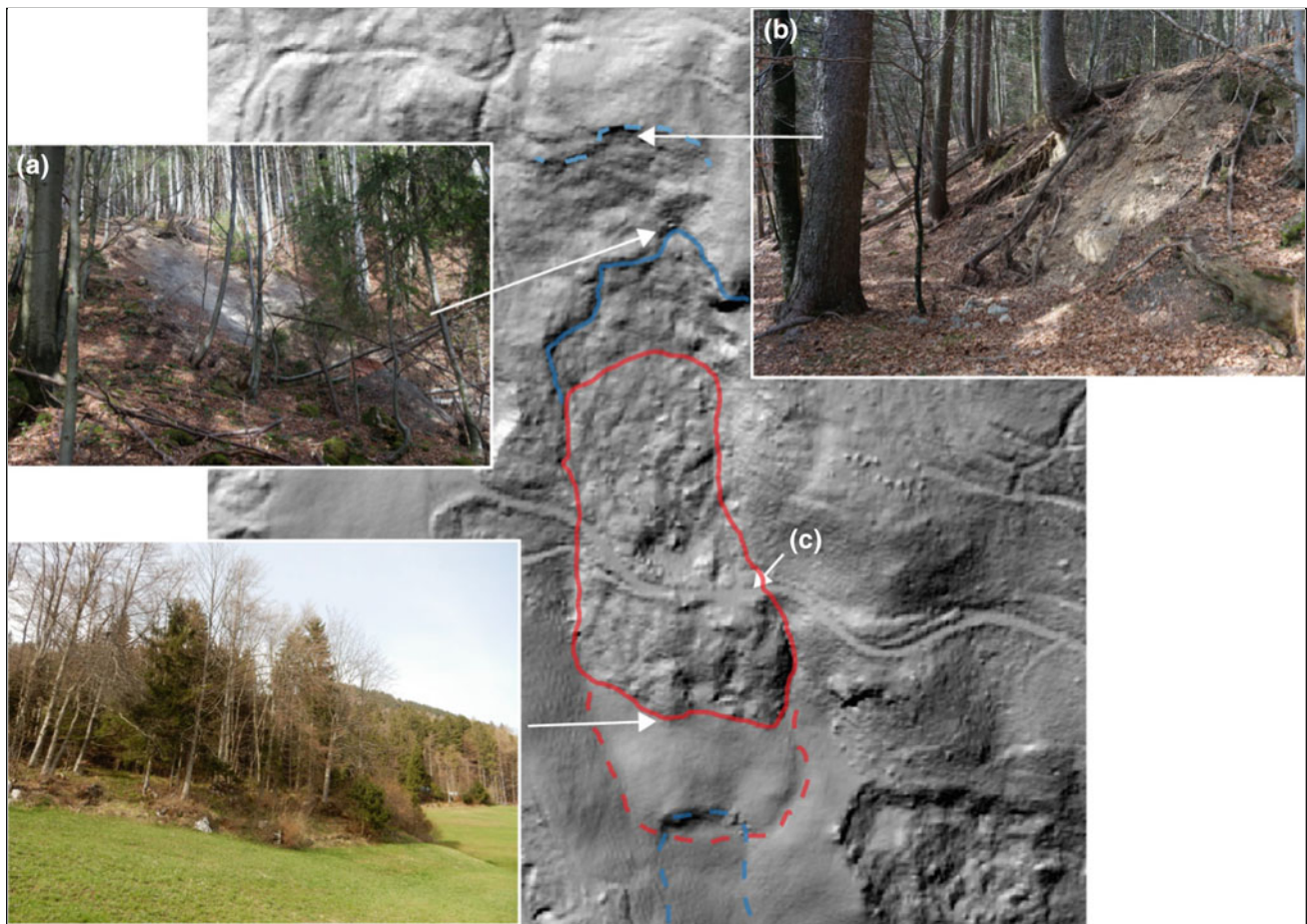


Fig. 5 Hillshade view of a landslide with field photographs of key locations

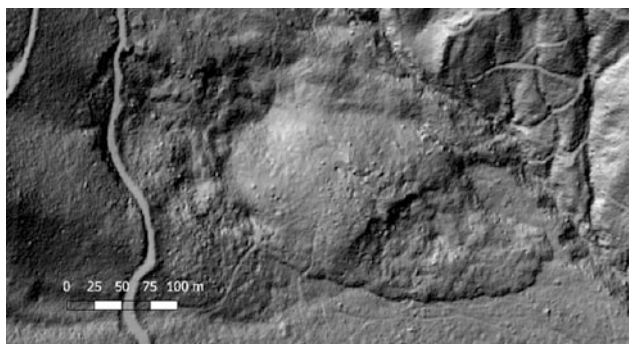


Fig. 6 A clearly defined landslide that was later found to be inactive

Conclusions

The present work is one of the first attempts of landslide inventory mapping in an area covered by forest in Slovenia. Altogether 114 landslides were mapped using Lidar-derived hillshades, correlated with PSInSAR data and the landslide database, and a limited sample was later checked in the field. Field validation was limited due to inaccessible terrain

covered by forest and altered by human actions. Given the small random number of checked landslides in the field it follows that Lidar data can be used for landslide identification of prehistoric landslides that are now covered by vegetation. To identify shallow landslides and slips of smaller dimensions, typically triggered during the heavy rainfall as prevail in the study area, Lidar DEM can be only used complementary with other techniques.

One of the limitations of the method is also its subjectivity and dependence on the expertise of the person carrying out the mapping. But with a better perspective on the correlation of landforms visible on hillshades and in the field the method will certainly improve our ability to produce accurate and dependable landslide inventory maps. At the moment, we see little chance of automatizing the process, as it is hard to objectively identify the landforms indicative of landsliding, especially for slope instabilities of smaller dimensions.

Acknowledgements Authors would like to thank Slovenian Research Agency for founding Programme of Regional Geology (P1-0011) within which the study was conducted.

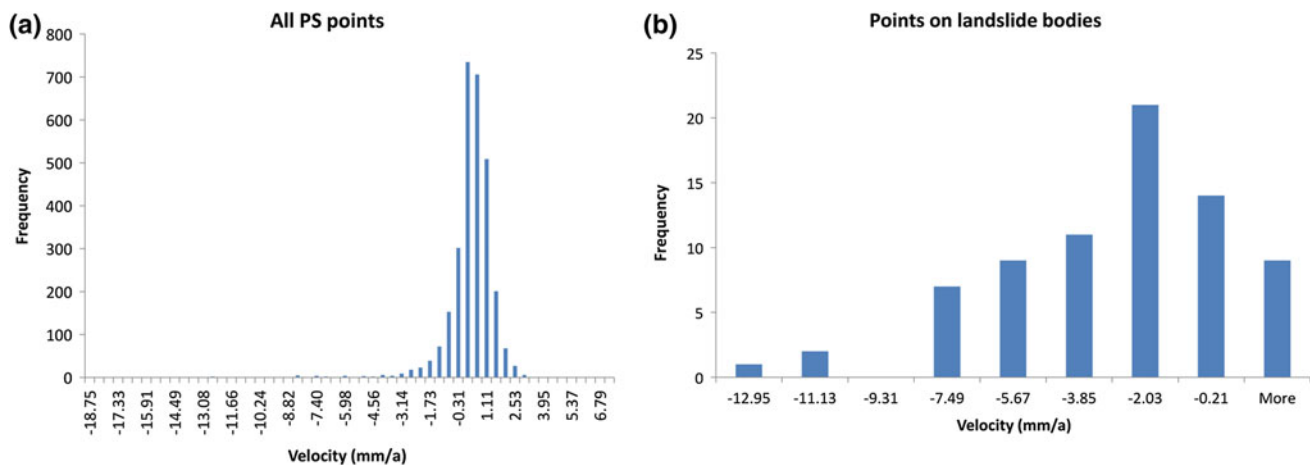


Fig. 7 Distributions of PSInSAR velocities for **a** all PS points and **b** points located on landslide bodies

References

- Annual reports from 1991 to 2010. Administration for civil protection and disaster relief. Ljubljana
- Buser S, Cimerman F, Dozet S, Ferjančič L, Grad K, Mioč P, Premru U, Vujič D, Žlebnič L, Žnidarčič M (1968) Osnovna geološka karta Socialistične Federativne Republike Jugoslavije 1:100.000, L 33–65 Kranj. Geološki zavod Ljubljana, Ljubljana
- Colesanti C, Ferretti A, Novali F, Prati C, Rocca F (2003) SAR monitoring of progressive and seasonal ground deformation using the permanent scatterers technique. *IEEE TGRS* 41(7):1685–1701
- Crosetto M, Monserrat O, Cuevas-González M, Devanthery N, Crippa B (2016) Persistent scatterer interferometry: a review. *ISPRS J Photogramm Remote Sens* 115:78–89. doi:10.1016/j.isprsjprs.2015.10.011
- Čarman M, Jemec Auflič M, Komac M (2014) Landslides at a uranium mill tailing deposit site Boršt (Slovenia) detected by radar interferometry. *Landslides* 11(3):527–536. doi:10.1007/s10346-013-0454-9
- Ferretti A, Prati C, Rocca F (2001) Permanent scatterers in SAR interferometry. *IEEE Trans Geosci Remote Sens* 39(1):8–20
- Glenn NF, Streutker DR, Chadwick DJ, Thackray GD, Dorsch SJ (2006) Analysis of LiDAR derived topographic information for characterizing and differentiating landslide morphology and activity. *Geomorphology* 73(1–2):131–148
- Guzzetti F, Mondini AC, Cardinali M, Fiorucci F, Santangelo M, Chang KT (2012) Landslide inventory maps: new tools for an old problem. *Earth Sci Rev* 112(1–2):42–66
- Jaboyedoff M, Oppikofer T, Abellán A, Derron MH, Loye A, Metzger R, Pedrazzini A (2012) Use of LiDAR in landslide investigations: a review. *Nat Hazards* 61(1):5–28
- Jemec Auflič M, Kumelj Š, Prkić N, Šinigoj, J (2015) Zbiranje podatkov o zemeljskih plazovih in zanesljivost napovedovanja njihovega proženja = Landslide data collection and evaluation of predicted models. *Ujma*, ISSN 0353-085X, 29:363–370
- Jemec Auflič M (2012) Uporaba metode permanentnih sipalcev v geologiji kot podpora pri proučevanju plazljivih območij. PhD thesis, University of Ljubljana, Ljubljana
- Jemec Auflič M, Komac M (2013) Rainfall patterns for shallow landsliding in perialpine Slovenia. *Nat Hazards* 67(3):1011–1023. doi:10.1007/s11069-011-9882-9
- Jemec Auflič M, Mikoš M (2008) Slope mass movements on SPOT satellite images: a case of the Železniki area (W Slovenia) after flash floods in September 2007. *Geologija* 51(2):235–243
- Kasai M, Ikeda M, Asahina T, Fujisawa K (2009) LiDAR-derived DEM evaluation of deep-seated landslides in a steep and rocky region of Japan. *Geomorphology* 113(57–69). doi:10.1016/j.geomorph.2009.06.004
- Komac M, Fajfar D, Ravnik D, Ribičič M (2007) Slovenian national landslide database—a promising approach to slope mass movement prevention plan. *Geologija* 50(2):393–402
- Li X, Cheng X, Chen W, Chen G, Liu S (2015) Identification of forested landslides using LiDAR data, object-based image analysis, and machine learning algorithms. *Remote Sens* 7:9705–9726
- Liu JK, Hsiao KH, Shih PTY (2012) A geomorphological model for landslide detection using airborne LiDAR data. *J Mar Sci Technol* 20(6):629–638
- McKean J, Roering J (2004) Objective landslide detection and surface morphology mapping using high resolution airborne laser altimetry. *Geomorphology* 57:331–351
- Podobnikar T (2005) Production of integrated digital terrain model from multiple datasets of different quality. *Int J Geogr Inf Sci* 19(1):69–89
- Popit T, Verbovšek T (2013) Analysis of surface roughness in the Sveta Magdalena paleo-landslide in the Rebrnice area Analiza hrapavosti površja fosilnega plazov Sveta Magdalena na območju Rebrnic. *RMZ Mater Geoenviron* 60(3):197–204
- Popit T, Kokalj Ž, Verbovšek T (2013) Lidar v geologiji in njegova uporaba pri prepoznavanju fosilnih plazov. *Življenje in tehnika* 64(5):66–74
- Popit T, Rožič B, Kokalj Ž, Šmuc A, Verbovšek T, Košir A (2014) A LiDAR, GIS and basic spatial statistic application for the study of ravine and palaeo-ravine evolution in the upper Vipava valley, SW Slovenia. *Geomorphology* 204:638–645
- Razak K A, Bucksh A., Damen M, Westen C V, Straatsma M, De Jong S (2013) Characterizing tree growth anomaly induced by landslides using LiDAR. In: Margotini C, Canuti P, Sassa K

- (eds) *Landslide science and practice. Volume 1: landslide inventory and susceptibility and hazard zoning*
- Schulz WH (2004) *Landslides mapped using LIDAR imagery*, Seattle, Washington. U.S. Geological Survey Open-File Report 2004-1396
- Schulz WH (2006) *Landslide susceptibility revealed by LIDAR imagery and historical records*, Seattle, Washington. *Eng Geol* 89:67–87
- Triglav Čekada M, Bric V (2015) *Končan je project laserskega skeniranja Slovenije—The project of laser scanning of Slovenia is completed*. *Geodetski vestnik* 59(3):586–592
- Van Den Eeckhaut M, Poesen J, Verstraeten G, Vanacker V, Moeyersons J, Nyssen J, Van Beek L P H, Vandekerckhove L (2007) Use of LIDAR-derived images for mapping old landslides under forest. *Earth Surf Process Landf* 32:754–769. doi:[10.1002/esp.1417](https://doi.org/10.1002/esp.1417)
- Van Westen CJ, Castellanos E, Kuriakose SL (2008) Spatial data for landslide susceptibility, hazard, and vulnerability assessment: an overview. *Eng Geol* 10:112–131